Environmental Science and Pollution Research
https://doi.org/10.1007/s11356-021-16411-y

ECOTOX, AQUATIC AND TERRESTRIAL ECOTOXICOLOGY CONSIDERING THE SOIL: WATER CONTINUUM IN THE ANTHROPOCENE CONTEXT

Potential ability of tobacco (*Nicotiana tabacum* L.) to phytomanage an urban brownfield soil

Eliana Di Lodovico[1,2] · Lilian Marchand[2] · Nadège Oustrière[2] · Aritz Burges[2] · Gaelle Capdeville[2] · Régis Burlett[2] · Sylvain Delzon[2] · Marie-Pierre Isaure[3] · Marta Marmiroli[1] · Michel J. Mench[2]

Received: 12 May 2021 / Accepted: 4 September 2021

Abstract

The ability of tobacco (*Nicotiana tabacum* L. cv. Badischer Geudertheimer) for phytomanaging and remediating soil ecological functions at a contaminated site was assessed with a potted soil series made by fading an uncontaminated sandy soil with a contaminated sandy soil from the Borifer brownfield site, Bordeaux, SW France, at the 0%, 25%, 50%, 75%, and 100% addition rates. Activities of sandblasting and painting with metal-based paints occurred for decades at this urban brownfield, polluting the soil with metal(loid)s and organic contaminants, e.g., polycyclic aromatic hydrocarbons, in addition to past backfilling. Total topsoil metal(loid)s (e.g., 54,700 mg Zn and 5060 mg Cu kg^{-1}) exceeded by seven- to tenfold the background values for French sandy soils, but the soil pH was 7.9, and overall, the 1M NH_4NO_3 extractable soil fractions of metals were relatively low. Leaf area, water content of shoots, and total chlorophyll (Chl) progressively decreased with the soil contamination, but the Chl fluorescence remained constant near its optimum value. Foliar Cu and Zn concentrations varied from 17.8 ± 4.2 (0%) to 27 ± 5 mg Cu kg^{-1} (100%) and from 60 ± 15 (0%) to 454 ± 53 mg Zn kg^{-1} (100%), respectively. Foliar Cd concentration peaked up to

Highlights
- Total soil Zn, Cu, and Pb were high, but their bioavailability was low.
- Quartz, calcite, microcline, fayalite, wüstite, magnetite/maghemite, Fe silicates, metallic Fe, and Zn and Cu chromite were detected in the brownfield soil.
- This tobacco cultivar grew relatively well in the brownfield soil.
- Leaf area, water content of shoots, foliar total chlorophyll, and hydraulic efficiency of stem progressively decreased with the soil contamination.
- Tobacco can annually phytoextract a fraction of the bioavailable soil Zn and Cd.

Responsible Editor: Elena Maestri

✉ Michel J. Mench
michel.mench@inrae.fr

Eliana Di Lodovico
elidilod@gmail.com

Lilian Marchand
marchand.lilian@gmail.com

Nadège Oustrière
oustriere.nadege@gmail.com

Aritz Burges
aburges82@gmail.com

Gaelle Capdeville
gaelle.capdeville@inrae.fr

Régis Burlett
Regis.Burlett@U-Bordeaux.Fr

Sylvain Delzon
sylvain.delzon@u-bordeaux.fr

Marie-Pierre Isaure
marie-pierre.isaure@univ-pau.fr

Marta Marmiroli
marta.marmiroli@unipr.it

[1] Univ. Parma, via Universita 12, 43121 Parma, Italy

[2] Univ. Bordeaux, INRAE, BIOGECO, Bât. B2, Allée Geoffroy St-Hilaire, CS50023, F-33615 Pessac cedex, France

[3] Univ. Pau et Pays de l'Adour, E2S UPPA, CNRS, IPREM-UMR 5254, Hélioparc, 2 Avenue Pierre Angot, F-64053 Pau cedex9, France

Published online: 18 October 2021

1.74 ± 0.09 mg Cd kg^{-1}, and its bioconcentration factor had the highest value (0.2) among those of the metal(loid)s. Few nutrient concentrations in the aboveground plant parts decreased with the soil contamination, e.g., foliar P concentration from 5972 ± 1026 (0%) to 2861 ± 334 mg kg^{-1} (100%). Vulnerability to drought-induced embolism (P50) did not differ for the tobacco stems across the soil series, whereas their hydraulic efficiency (Ks) declined significantly with increasing soil contamination. Overall, this tobacco cultivar grew relatively well even in the Borifer soil (100%), keeping its photosynthetic system healthy under stress, and contaminant exposure did not increase the vulnerability of the vascular system to drought. This tobacco had a relevant potential to annually phytoextract a part of the bioavailable soil Zn and Cd, i.e., shoot removals representing here 8.8% for Zn and 43.3% for Cd of their 1M NH_4NO_3 extractable amount in the potted Borifer soil.

Keywords Cadmium · Metal · Organic contaminant · Phytoremediation · Phytoextraction · Zinc

Abbreviations

PAH	Polycyclic aromatic hydrocarbons
PCB	Polychlorinated biphenyls
BTEX	Benzene, toluene, ethylbenzene, and xylenes

Introduction

Despite some progress made in the management of contaminated sites by EU Member States and cooperating countries, the use of phytotechnologies to remediate contaminated brownfield soils is still not widespread (Payá-Pérez and Peláez-Sánchez 2017). Increasing the frequency of their use remains a huge task. The US EPA listed 9 million ha of possibly contaminated land and 1327 abandoned, worst hazardous waste sites on its National Priority List (USEPA 2021). Chinese contaminated soils would reach 20 million ha (Sun et al. 2019). Urban brownfields represent at least 150,000 ha in France. Between 2010 and 2016, 95 sites have been remediated (65 completed, 30 in progress) by the French agency of ecological transition, representing 491 ha (ADEME et al. 2018). The lack of specific policy instruments and guidelines on the reuse of contaminated soils can impede sustainable remediation even in countries with well-developed policies and regulatory frameworks (Reinikainen et al. 2016; Moreira et al. 2021). In parallel, prospects and threats regarding future land use, e.g., options of site redevelopment and the potential long-term liabilities, in line with economic and social uncertainties, influence the strategy for risk management and the desired remediation level, the trend being to do more than required after risk assessment (Bardos et al. 2020; Moreira et al. 2021). Progress toward sustainable land management of contaminated soils is driven by several generic elements: e.g., increased recognition of environmental impacts and benefits of remediation, stakeholders' demand for more sustainable practices, lack of regulatory requirements, economic considerations, and institutional pressure that promotes sustainable practices (Hou et al. 2014; Rizzo et al. 2016; Bardos et al. 2018, 2020). The European Parliament has just adopted a resolution in this way for the soil protection and the remediation of contaminated soils (European Parliament 2021).

Two main priorities for the topic of phytoremediation and phytomanagement of polluted soils are (1) to guide the collection of case study data for identifying and assessing methods and (2) to develop tools to guide remediation of soil ecological functions underlying ecosystem services (Macci et al. 2020). Indeed, each brownfield site has specific environmental challenges and management plan. With this in mind, the Borifer brownfield site is a part of the Parc aux Angéliques located in the Bordeaux downtown, south-west France, with contaminated soil requiring remediation. The topsoil is mostly barren at the Borifer site, due to anthropogenic soil contamination by metal(loid)s and organic xenobiotics, soil compaction, low fertility, and low water-holding capacity (Marchand and Mench 2015). Some vegetation patches are colonizing this brownfield. Thirty-one plant species were identified in May 2018, *Bromus sterilis* L. and *Vulpia myuros* (L.) C.C.Gmel. being dominant. Most of plant colonists had a low shoot biomass, and at several patches, plants displayed some visible symptoms of phytotoxicity (e.g., leaf chlorosis, dwarfism, and sometimes purple coloration on aboveground plant parts). After soil loosening, a temporary phytomanagement could cover the soil surface, prevent dust from flying, stimulate the xenobiotic biodegradation, mitigate metal(loid) migration with natural agents, and improve soil properties. This would correspond with a future land use to complete a green corridor on the right bank of the Garonne River, crossing the Bordeaux downtown. High total soil Cu and Zn and many organic contaminants were evidenced in the Borifer topsoils (Table 1, Marchand and Mench 2015). This can affect the microbial community decreasing its density, diversity, and vitality, especially due to the toxicity of the Cu ionic form (Cu^{2+}) (Bourceret et al. 2018; Xue et al. 2018). Soil Zn- and Cu-contamination can affect plant growth as well (Chaney 1993; Verdejo et al. 2016; Küpper and Andresen 2016; Kolbas et al. 2018).

Relevant tools to remediate and contain soil contamination include the Gentle Remediation Options (GRO), which aim at reducing the pollutant linkages through transformation, stabilization, degradation, or extraction of contaminants using fungi (myco-), plant (phyto-), and/or bacteria-based methods, with or without

Table 1 Main physico-chemical properties of the control (0%), faded and Borifer (B, 100%) soils

Soil parameters	Control soil (0%)	25%	50%	75%	B soil (100%)	French sandy soils
pH	7.9	7.9	7.9	7.9	7.9	7.35*
Organic C (g/kg)	40.4	34.9	29.5	24.1	18.7	14.5 (12*)
Total N (g/kg)	2.94	2.32	1.71	1.10	0.49	1.45 (0.55*)
C/N	13.8	15.0	17.2	21.9	38.2	10.0 (21.8*)
Organic matter (g/kg)	69.9	60.5	51.1	41.8	32.4	14.6 (8–20)
CEC (cmol+/kg)[1]	16.1	12.4	8.7	5.0	1.3	5*
Total $CaCO_3$ (g/kg)	5	21	37	53	69	
Extractable soil P_2O_5 (g/kg)[2]	0.151	0.142	0.135	0.127	0.120	
Cd (mg/kg)	0.27	2.36	4.45	6.54	8.64	
Cu (mg/kg)	21.5	1281	2540	3800	5060	3.2–8.4
Co (mg/kg)	2.8	105	208	310	413	
Cr (mg/kg)	17.9	708	1399	2089	2780	14–40
Hg (mg/kg)	< 0.1	< 0.1	< 0.1	< 0.1	< 0.1	
Ni (mg/kg)	7.46	80	153	225	298	4.2–14.5
Pb(mg/kg)	24.4	741	1457	2173	2890	
Zn (mg/kg)	50.9	13,713	27,375	41,037	54,700	17–48
Tl (mg/kg)	nd	nd	nd	nd	0.75	
Mo (mg/kg)	1.43	52	102	152	203	
Al (mg/kg)	6780	12,285	17,790	23,295	28,800	
B (mg/kg)	nd	nd	nd	nd	619	
Ba (mg/kg)	41.6	521	1000	1480	1960	
Ca (mg/kg)	10,424	21,843	33,262	44,681	56,100	
Fe (mg/kg)	6940	64,455	121,970	179,485	237,000	6000–14,300
K (mg/kg)	1879	2841	3804	4767	5730	
Mg (mg/kg)	1253	2714	4176	5638	7100	
Mn (mg/kg)	214	898	1582	2266	2950	72–376
Na (mg/kg)	54	2340	4627	6913	9200	
P_2O_5 (mg/kg)	nd	nd	nd	nd	3000	
As (mg/kg)	3.62	23.5	43.5	63.4	83.4	
Bi (mg/kg)	0.17	1.12	2.08	3.04	4.0	
In (mg/kg)	<0.10	1.27	2.45	3.62	4.8	
Se (mg/kg)	0.23	2.17	4.11	6.05	8.0	
Sb (mg/kg)	0.43	22.9	45.4	67.9	90.4	
Sn (mg/kg)	0.83	111	223	334	445	
Extractable Cd (mg/kg)[3]	< 0.001	0.004	0.008	0.0129	0.0173	
Extractable Cu (mg/kg)[3]	0.266	4.15	8.03	11.91	15.80	
Extractable Pb (mg/kg)[3]	< 0.005	0.008	0.013	0.018	0.023	
Extractable Zn (mg/kg)[3]	0.042	6.5	13.0	19.5	26.0	
Extractable Cr (mg/kg)[3]	< 0.015	< 0.015	< 0.015	< 0.015	< 0.015	
Extractable Ni (mg/kg)[3]	0.009	0.099	0.190	0.281	0.372	
(Total) cyanides (mg/kg)[4]	< 0.5	< 0.5	< 0.5	< 0.5	< 0.5	

All units in soil DW; *Fluviosol soil series in the Gironde county, France; [1] Cobaltihexamine method, ISO 23470; [2] Olsen method, NF ISO 11263; [3] 1M NH_4NO_3 extractable soil fraction; [4] NF EN ISO/IEC 17025:2005

nd not determined

amendments or chemical additives (Cundy et al., 2016). Cultivation of fibrous, aromatic, and other non-food crops is an option, e.g., flax (*Linum usitatissimum* L.), jute (*Corchorus capsularis* L.), hemp (*Cannabis sativa* L.), ramie (*Boehmeria nivea* (L.) Gaudich., kenaf (*Hibiscus cannabinus* L), nettles (*Urtica dioïca* L.),

clary sage (*Salvia sclarea* L.), coriander (*Coriandrum sativum* L.), and tobacco (*Nicotiana tabacum* L.)) (Rehman et al. 2019; Jeannin et al. 2020; Saleem et al. 2020a,b; Moreira et al. 2021). More specifically, in the climatic conditions of southwest and central Europe, several plant species (e.g., *N. tabacum* L., *Helianthus annuus* L., *Miscanthus x giganteus* J.M. Greef & Deuter ex Hodk. & Renvoize, *Chrysopogon zizanioides* (L.) Roberty, *Agrostis capillaris* L., *Agrostis gigantea* Roth, *Populus nigra* L., *Salix caprea* L., *Brassica juncea* (L.) Czern., *Erucastrum incanum* (L.) W.D.J. Koch, and *Amorpha fruticosa* L.) are able to relatively tolerate root exposure to Cu and Zn excess, polycyclic aromatic hydrocarbons (PAHs), and other xenobiotics, while producing a valuable biomass (Herzig et al. 2014; Kidd et al. 2015; Kolbas et al. 2018, 2020; Mench et al. 2017, 2018; Ndubueze 2018). Tobacco is a plant species frequently evaluated in Western Europe and also in China for phytomanaging contaminated soils because it can extract and store metals in its tissues: Zn and Cd in the shoots and Cu and Pb mainly in the roots (Herzig et al. 2014; Thijs et al. 2018; Yang et al. 2017; Rehman et al. 2019; Moreira et al. 2021). It can stimulate the biodegradation of organic xenobiotic by the rhizosphere microorganisms (Rezek et al. 2004; Azaizeh et al. 2011; Prouzova et al. 2012; Bisht et al. 2015; Petrová et al., 2017). Processes that valorize tobacco biomass were reported by Asad et al. (2017), Yang et al. (2017), Rehman et al. 2019, and Kolbas et al. (2020), e.g., pyrolysis, hydrothermal oxidation, fermentation, and gasification. The main objectives to be reached by the soil phytomanagement using tobacco at the Borifer site would be to progressively remove the phytoavailable soil Cd and Zn by harvesting shoots, to immobilize in the roots the phytoavailable fraction of several metal(loid)s, e.g., Cu and Pb, to stimulate the dissipation of organic pollutants through the rhizodeposition and microbial biodegradation, and to improve soil properties, e.g., sequestration of carbon. Consequently, this study aimed at assessing the ability of tobacco to grow on a potted soil series with an increasing proportion of the contaminated soil of the Borifer site, to evaluate its behavior toward metal(loid)s in this sandy soil with mixed contamination, and to assess its vulnerability to drought-induced embolism in such soil conditions as periods of intense spring and summer droughts become more frequent with climate change. In addition to the characterization of soil properties, fresh weight (FW) and dried weight (DW) biomass of aboveground plant parts, leaf area (LA), vulnerability to drought-induced embolism (P50) and hydraulic efficiency (Ks) of tobacco stems, the foliar and stem ionomes (Salt et al. 2008), pigment content, and chlorophyll fluorescence of the leaves were determined.

Materials and methods

Site history

The former Borifer site (44° 51′ 08.6″ N, 0° 33′ 29.5″ W, altitude 15 m) is located in the Bordeaux downtown (Gironde County, South-West France), on the right bank of the Garonne River, near the Parc aux Angéliques and Chaban-Delmas Bridge (Fig. 1). At this site (1.1 ha), activities of sandblasting with abrasive glass and iron grits and painting with metal-based paints of detached metallic pieces and naval parts took place for decades (Marchand and Mench 2015). A historical soil contamination is also due to the backfilling of the Garonne River banks. The bedrock is constituted by the Mattes clays, these bluish to grayish clays with peaty past being present on both sides of the Garonne River. Since the City of Bordeaux decided to include this site in the urban park, the soil analysis was performed showing high concentrations of metal(loid)s and xenobiotics (PAH, PCB, aliphatic hydrocarbons, etc.) (Marchand and Mench 2015, Table S1). The soil texture is sandy and the metal(loid) concentrations in the topsoil largely exceed (seven- to tenfold) the background values for French sandy soil, depending on the plots.

Soil series

The Borifer soil (B) was collected (100 kg DW) in the 0–30-cm depth layer of the S41 plot. It is mainly sandy backfill with pebbles. The uncontaminated control soil (Ctrl) was sampled in a kitchen garden, Gradignan, France. Both sandy soils were air-dried and sieved at 4 mm. Soil texture and physico-chemical parameters were determined with standard methods and a quality scheme by INRA LAS (2018), Arras, France, i.e., inductively coupled plasma/atomic emission spectroscopy (ICP-AES) for metals after wet digestion (HF and $HClO_4$) and hydride-generation for As after wet digestion in H_2SO_4/HNO_3 (2/1) with V_2O_5 at 100 °C (3 h).

Soil particles were separated into a light (44% of the soil mass) and heavy (56% of the soil mass) fractions by densimetry using a sodium polytungstate liquor with a density of 2.9 (Morgun and Makarov, 2011). Samples were ground and sieved at 100 μm. In the bulk soil, a fraction was non-crushable and was composed of shiny metallic and black particles (Fig. 2A). These non-crushable particles were separated into a magnetic fraction including ferromagnetic/ferrimagnetic phases and a non-magnetic fraction using a hang magnet (Fig. 2B, C). The bulk soil and fraction mineralogy was investigated by X-ray diffraction (XRD) using a D2 diffractometer (Brucker) operating with a Cu Ka source. X-ray

Fig. 1 Aerial view of the Borifer site location. (source: https://api.mapbox.com/styles/v1/mapbox/satellite-v9/static/-0.559479399756782,44.852388436311344,17.187273764169767,0.00,0.00/1280x1280@2x?access_token=pk.eyJ1IjoiY3licml3c2t5IiwiYSI6ImNqd2tmbndrejBjdDQzeXBqaTNqZzYzMjYifQ.uit0M0u2n8w-585Ck_rs9Q)

powder diffraction patterns were recorded from 5 to 90° 2θ with a 0.02° step and a 5-s counting time per point. Soil properties are given in Tables 1 and 2. The Borifer soil was faded with the Ctrl soil, at rates varying from 0% (Ctrl) to 25% (B25), 50% (B50), 75% (B75), and 100% (B), and filled (1000 g air-dried soil) in plastic pots, with four replicates. Potted soils were irrigated with tap water, and let to react for 2 weeks (60% soil humidity, laboratory conditions).

Plant growth and measurements

The tobacco plants cv. Badischer Geudertheimer (BaG) were firstly sowed and grown in the Ctrl soil under a greenhouse for 4 months. One plant was thereafter transplanted in each pot containing various proportions of Borifer soil on July 8. Pots were randomly placed in a laboratory with glass wall (due to the Covid 19 lockdown and to prevent heatwaves, the greenhouses being not daily accessible), their position being changed every 2–3 days. From the first-day, maximum shoot length (height), the number of leaves, and chlorophyll content (chlorophyll meter "Opti-sciences CCM-200") were determined. The measurements were taken in days 1, 23, 41, 51, and 64 for following the development of the leaf stages. On day 23, some mineral NPK fertilizers were added (Blaukorn classic, 12–8–16 (3–25)) at 40 kg N (58% NH_4, 42% NO_3), 26.7 kg P_2O_5, 53 kg K_2O, 10 kg MgO, 83 kg SO_3, 0.06 kg B, 0.2 kg Fe, and 0.04 kg Zn per ha. The plants were daily watered (up to 70% of the water holding capacity) considering few aspects: the soil water capacity (10% of the soil total weight), tobacco evapotranspiration, and the increase of 5-g fresh weight (FW)/plant/week due to the gain in biomass. Between the 3rd and the 4th weeks from the transplantation day, the plants started to show the effects of the contaminant exposure with some leaves displaying interveinal discoloration (plants grown in the B soil). On the days 57 and 62, the plants were placed in a dark room overnight, and the chlorophyll fluorescence was measured (Chlorophyll fluorometer PAM-210 Walz, Germany) in the morning before the sunrise. The minimal fluorescence level in the dark-adapted state (F_0) was measured using a modulated pulse (<0.05 μmol m^{-2} s^{-1} for 1.8 μs). Maximal fluorescence in this state (*Fm*) was measured after applying a saturating actinic light pulse of 15,000 μmol m^{-2} s^{-1} for 0.7 s. The value of *Fm* was recorded as the highest average of four consecutive points. Values of variable fluorescence ($Fv = Fm - F_0$) and maximum quantum efficiency of PSII photochemistry (*Fv*/*Fm*) were calculated from F_0 and *Fm*. This *Fv*/*Fm* ratio correlates with the number of functional PSII reaction centers, and dark-adapted values of *Fv*/*Fm* can be used to quantify photoinhibition (Cambrollé et al. 2012).

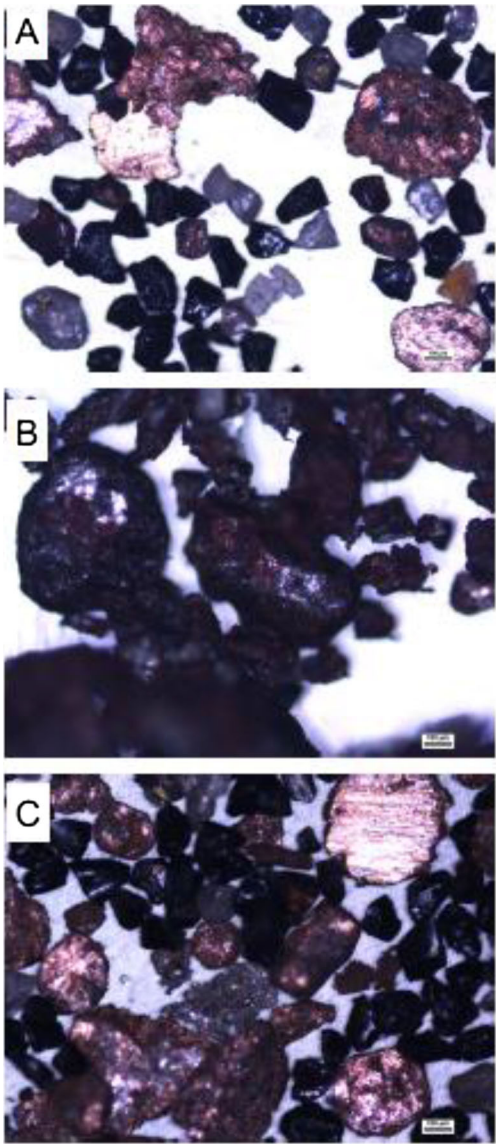

Fig. 2 Optical microscopy images of bulk soil (**A**), magnetic non-crushable soil fraction (**B**), and non-magnetic non-crushable soil fraction (**C**)

Plant parameters and laboratory operations

Fresh and dried weight

At sampling time (day 66), all leaves and stems were weighed for determining their total fresh weight (FW). After measuring the plant traits, plant parts were washed in MilliQ water and put in a ventilated oven (50°C, till constant weight) to determine the total dried weight (DW). Fresh stem samples were kept to determine their vulnerability to drought-induced embolism and hydraulic conductivity (see below). Plant samples were labeled according to the soil treatments and the addition rate of B soil (i.e., Ctrl, B25, B50, B75, and B).

Pigments content

Four discs (0.8-cm diameter, giving 1 cm^2 in duplicate) were taken at the mid-length of the 6th leaf (starting from the top) of each plant, from both mid-rib sides. Two discs were placed in 3 mL cold DMF (N,N-dimethylformamide) (in duplicate). The extraction lasted 48h at 4°C, then the content of chlorophyll A, B, and carotenoids was computed after measuring the absorbance at 470, 664, and 647 nm with a spectrophotometer (Libra S22 of Biochrom). Formulae and extinction coefficients for computing chlorophyllous pigments were published by Lichtenhaler and Wellburn (1983), and Blanke (1990).

Leaf area

All the leaves were cut from the plants and placed between filter papers. Each leaf was labeled with the treatment, the replicate number, and the leaf number. The leaves nos. 4, 8, and 9 of each plant were used to determine the leaf surface using a scanner (Epson Expression 10000 XL) and the WinFOLIA software.

Vulnerability to cavitation

The plant stems were used to characterize the vulnerability to drought-induced embolism at the Caviplace laboratory (PHENOBOIS platform, INRAE-University of Bordeaux, France) with the Cavitron technique (Cochard et al. 2005). Centrifugal force was used to establish negative pressure in the xylem and to provoke water stress-induced cavitation, using a custom-built honeycomb rotor (DGMeca, Gradignan, France) mounted on a high-speed centrifuge (Sorvall RC5 plus, MSE Scientific, London, UK). This technique enables to measure both the hydraulic conductance of a branch under negative pressure and the vulnerability of stem xylem to water stress-induced embolism caused by air seeding (Delzon et al. 2010). Each stem was cut at the base, the foliage removed, then wrapped in a wet cloth and placed in a plastic bag to maintain it hydrated with a high moisture level. The stems were then stored in a fridge at 5°C before carrying on the vulnerability to embolism measurements. Prior to measurement, stems were re-cut under water to a standard length of 27 cm. Samples were infiltrated with a reference ionic solution of 10 mM KCl and 1 mM $CaCl_2$ in deionized ultrapure water. Centrifugal force was used to generate negative pressure into the xylem and induce cavitation. Maximum conductance of stem (K_{max} in m^2 MPa^{-1} s^{-1}) was calculated under low xylem pressures (close to zero) (P in MPa). Then, rotation speed of the centrifuge was gradually increased by 0.5 or 1 MPa, to lower xylem pressure. The percentage loss of hydraulic conductance (PLC) of the stem was determined at each pressure step to build a vulnerability curve corresponding to

Table 2 Concentrations of organic contaminants in the Borifer soil (B soil, values in bold exceeded the environmental health guideline value for agricultural land use)

mg/kg soil DW	**B soil**	**French agricultural soils**[3]	**Environmental health guideline values**[4]		
			A	**B**	**C**
			Soil and food ingestion Interim soil quality criteria (or *Soil Quality Guideline* [5])		
Naphthalene	0.0903		8.8 0.6	8.8 0.6	22
Acenaphthene	0.0612		21.5 -	21.5 -	
Fluorene	0.0421		15.4 -	15.4 -	
Phenanthrene	0.48	0.007	43 0.1	43 5	50
Anthracene	0.076		61.5 *2.5*	61.5 *2.5*	*32*
Fluoranthene	10.2	0.007	15.4 *50*	15.4 *50*	*180*
Pyrene	0.831	0.007	7.7 0.1	7.7 10	100
Benzo(a)anthracene	0.617		6.2 0.1	6.2 1	10
Chrysene	0.667		6.2 -	6.2 -	
Benzo(b)fluoranthene	0.776	0.006	6.2 0.1	6.2 1	10
Benzo(k)fluoranthene	0.394		6.2 0.1	6.2 1	10
Benzo(a)pyrene	0.689		0.6 *20*	0.6 *20*	*72*
Dibenzo(a,h)anthracene	0.286		- 0.1	- 1	- 10
Benzo(g,h,i)perylene	0.765				
Indeno(123-c,d)pyrene	0.539		- 0.1	- 1	- 10
Acenaphthylene	0.0391				
∑ 16 PAH	16.55				
THC C10-C40	230				
THC nC10-nC16	12.7				
THC >nC16-nC22	63.3				
THC >nC22-nC30	101				
THC >nC30-nC40	53.6				
∑ PCB	0.23				
Benzene	< 0.05				
Toluene	< 0.05				
Ethylbenzene	< 0.05				
o-Xylene	0.14				
m+p -Xylene	0.18				
∑ BTEX	$0.32 < x < 0.47$				

[3] Villanneau et al. (2013); [4] Environment Canada (2010) Environmental health guidelines/check values based on non-carcinogenic effects of PAHs; [5] Land use: (A) agricultural, (B) residential/parkland, and (C) industrial; *THC*, total aliphatic hydrocarbons; *PCB*, polychlorobiphenyls

PLC versus xylem pressure (*P*) (Delzon et al. 2010). For each sample, a sigmoid function (Pammenter and Willigen, 1998) was fitted to the vulnerability curve using proc NLIN in SAS 9.4 according to the equation:

$$PLC = \frac{100}{1 + \exp\left(\frac{S}{25(Pi - P50)}\right)}$$

where P_{50} (MPa) is the xylem pressure inducing 50% loss of hydraulic conductance and S (% MPa^{-1}) is the slope of the vulnerability curve at the inflection point (Urli et al. 2013). The xylem pressures inducing 12% (P_{12}, xylem air entry point; MPa) and 88% (P_{88}; MPa) loss of hydraulic conductivity were calculated as follows: $P_{12} = 50/S + P_{50}$ and $P_{88} = -50/S + P_{50}$ (Urli et al. 2013). The specific hydraulic conductivity (Ks, m^2 MPa^{-1} s^{-1}) of the xylem was calculated by dividing the maximum hydraulic conductivity measured at low speed by the sapwood area of the sample. These parameters were averaged for tobacco plants of each soil treatment. After the measurements, stem samples were oven-dried and weighed.

ICP-MS analysis

Dried leaf and stem samples were ground (<1.0-mm particle size, Fritsch Pulverisette 19). Weighed aliquots (0.5 g DW) were put in TFM® (modified poly(tetrafluoroethylene) tubes with 5 mL suprapure 14 M HNO_3 and left overnight. Then, 2 mL 30% (v/v) H_2O_2 not stabilized by phosphates and 1 mL MilliQ water were added in each tube and samples wet-digested under microwaves (CEM Marsxpress 1200 W: from 0 to 10 min till 120°C, 11 to 15 min to reach 180°C, 15 min at 180°C, cooling during 1 h). Digested samples were filtered through ash-free papers (Dutscher 1440110B, porosity 5–8 μm) and adjusted to 100 mL with milliQ water. Certified reference material (BIPEA maize V463) and blank reagents were included in all series. Mineral composition (As, Ca, Cu, Cr, Fe, K, Mg, Mn, Na, Ni, P, and Zn) in digests was determined by ICP-MS (Thermo X series 200, INRAE USRAVE laboratory, Villenave d'Ornon, France). All elements were recovered (>95%) according to the standard values, and standard deviation for replicates was <5%. The bioconcentration factor (BCF) was computed as foliar element concentration vs. total soil element.

Statistical analysis

The shoot biomass, ionome, and all other plant parameters were tested using the one-way ANOVA (analysis of variance), and when significant differences occurred between the treatments, the post-hoc Tukey test was used to make multiple comparisons of mean values. Besides, a redundancy analysis (RDA) was performed, to make a multivariate comparison among all the parameters considered. Statistical analyses were performed using the R Project for Statistical Computing package 3.0.3 (Foundation for Statistical computing, Vienna, Austria). For the specific hydraulic conductivity, the Student-Newman-Keuls test and the REG procedure were used (SAS/STAT® 13.1).

Results and discussion

Soil properties (Tables 1 and 2)

The B soil displayed high metal(loid) concentrations, especially for Zn, Cu, Pb, Cr, and Ni, which largely exceeded their background concentrations in the French sandy soils and the French screening values (Table 1, Baize 1997). Only 0.3% of total soil Cu and 0.05% of total soil Zn were present in the 1M NH_4NO_3-extractable fraction of the B soil, likely due to metal speciation and alkaline soil pH. The extractable soil Zn exceeded the indicative value (0.5 mg Zn kg^{-1} that guarantees full soil fertility) of the Swiss soil protection act (Herzig et al. 2014). Extractable soil Pb and Cd were relatively low in the B soil. The Ctrl soil was not contaminated. Both soils had the same pH (7.9).

The bulk Borifer soil was mainly composed of quartz (SiO_2), calcite ($CaCO_3$), microcline ($KAlSi_3O_8$), fayalite (Fe_2SiO_4), wüstite (FeO), and potentially pyrite (FeS_2) (Fig. 3a). Densimetric and magnetic fractionation allowed to identify other crystallized minerals. In addition to fayalite and wüstite, magnetite (Fe_3O_4)/maghemite (Fe_2O_3) and zinc and copper chromite ($ZnCr_2O_4$ and $CuCr_2O_4$, respectively) were detected in the heavy fraction (Fig. 3b). The non-crushable magnetic fraction was composed of metallic iron and magnetite/maghemite present as black and reddish particles (Figs. 2B and 3c) while the non-magnetic fraction displayed $FeCu_4$ likely corresponding to the shiny golden particles observed in Fig. 2C. The identified metal-containing phases, i.e., metallic iron, iron silicates, and oxides as well as Zn, Cu chromite, and $FeCu_4$ likely resulted from materials used at the brownfield site for abrasion and painting. They suggested a low metal phytoavailability.

Organic C and total N contents were lower in the B soil than in the Ctrl soil, but similar to the values of the French Fluviosol soil series (Table 1; Richer de Forges 2020). The organic matter (OM) content and C/N value were high as compared to the French sandy soils (Baize 1997). The B soil was contaminated by PAH, fluoranthene, and then pyrene (to a lesser extent) being the major compounds (Table 2). For 8 out of 16 PAH chemicals, their concentration in the B soil exceeded the environmental health guideline values for agricultural land use regarding either soil quality guideline or soil and food ingestion based on non-carcinogenic effects (Table 2, Environment Canada 2010). However none exceeded the environmental health guideline value for a residential/parkland use. High soil OM in the B soil may restrict the PAH bioavailability (Harvey et al. 2002).

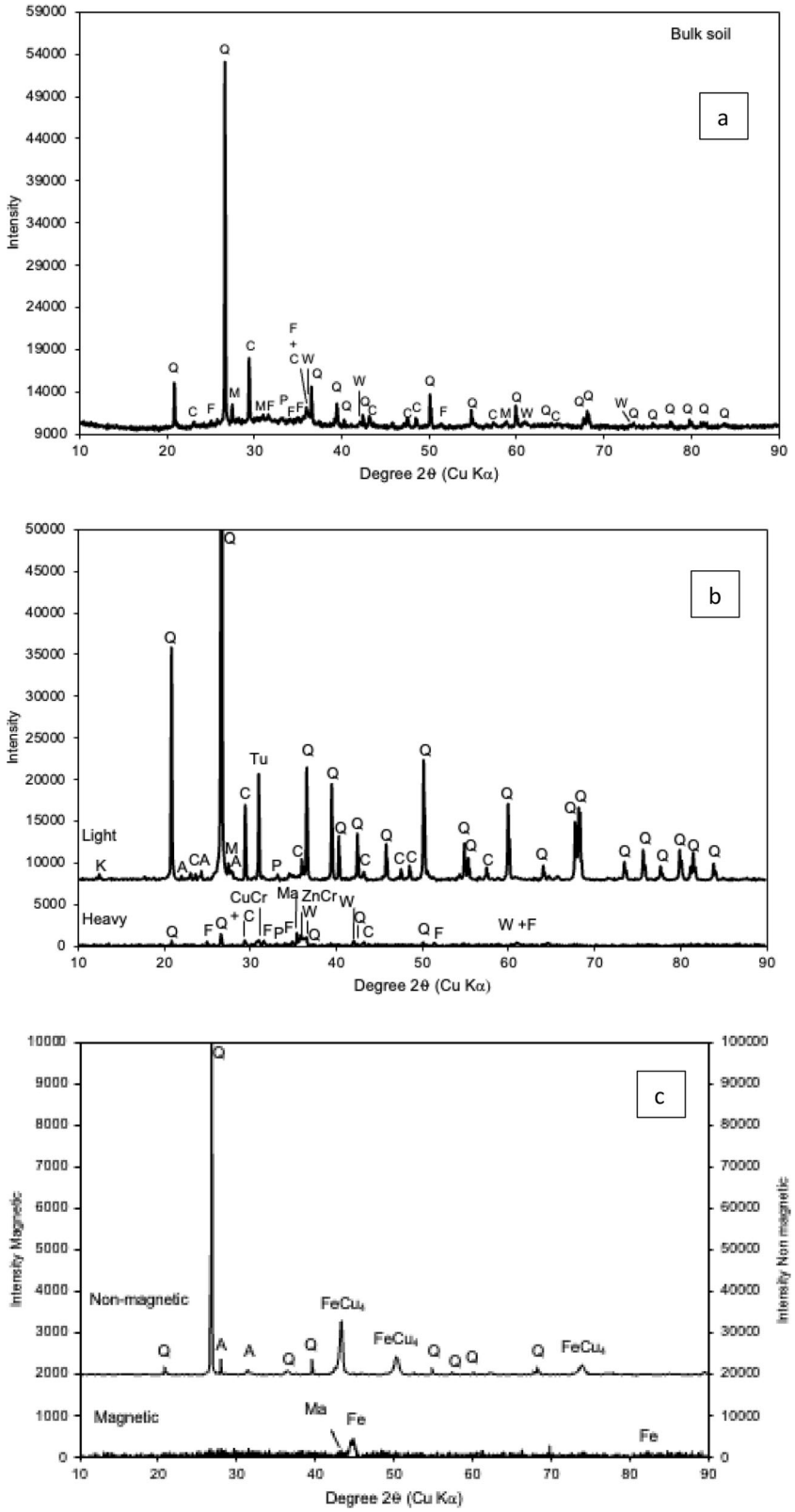

Fig. 3 **a** XRD pattern of the bulk Borifer soil. Detected phases were quartz (Q), calcite (C), microcline (M), fayalite (F), and wüstite (W). **b** XRD patterns of the heavy and light fractions of the Borifer soil. Detected phases were quartz (Q), calcite (C), microcline (M), albite (A), pyrite (P), and Ca tungsten oxide (Tu) originated from the liquor in the light fraction; and fayalite (F), wüstite (W), magnetite/maghemite (Ma), copper chromite (CuCr), and zinco chromite (ZnCr) in the heavy fraction. **c** XRD patterns of the magnetic and non-magnetic non-crushable fractions of the Borifer soil. Detected phases were metallic iron (Fe) and magnetite/maghemite (Ma) in the magnetic fraction and quartz (Q), albite (A), and $FeCu_4$ ($FeCu_4$) in the non-magnetic fraction

Table 3 Biometric parameters of the tobacco plants across the soil series

	Soil treatment (% of B soil)				
Plant parameters	**0**	**25**	**50**	**75**	**100**
Shoot DW yield (SDW, g DW plant^{-1})	8.9 ± 1.9 **a**	7.7 ± 0.8 **a**	7.5 ± 1.1 **a**	6.2 ± 0.9 **a**	5.9 ± 2.9 **a**
Stem biomass (g plant^{-1})	3.69 ± 1.01 **a**	3.24 ± 0.51 **a**	3.20 ± 0.68 **a**	2.40 ± 0.70 **a**	2.33 ± 1.57 **a**
H (cm)	49.4 ± 7.3 **a**	42.2 ± 1.8 **a**	43.4 ± 4.7 **a**	34 ± 6 **a**	33.5 ± 12.9 **a**
LA (cm^2)	136 ± 41 **a**	129 ± 43 **ab**	137 ± 37 **a**	124 ± 43 **ab**	93.4 ± 29.8 **b**
Number of leaves	17 ± 1 **a**	17 ± 2 **a**	15 ± 2 **a**	14 ± 2 **a**	15 ± 2 **a**
Water content of shoots (%)	78.4 ± 13.0 **a**	72.2 ± 5.8 **ab**	66.9 ± 6.4 **abc**	56.2 ± 8.0 **bc**	46.6 ± 13.0 **c**

H, maximum stem length; *LA*, leaf area

Values are means ± SD (n=4); letters indicate significant differences between treatments for each parameter at p <0.05 (post hoc Tukey HSD test)

Plant parameters

Biometric parameters

The shoot biomass (SDW), the maximum stem length (H), and the leaf area (LA) followed the same trend. They slightly decreased along with the increased proportion of contaminated B soil (Table 3), albeit this drop was only significant for the leaf area (−31% at 100% of B soil). The number of leaves did not significantly differ across the soil series. However some leaves displayed interveinal discoloration on their adaxial side for plants at the highest B soil rates. The water content of shoots significantly fell at the 75% and 100% addition rates of B soils (−28% and −40%, respectively). Despite the high contamination of the B soil, the impacts on the morphological parameters of tobacco plants were quite low. The plant exposure to PAHs can occur via particle-phase deposition on the waxy leaf cuticle and in the stomata, by the uptake from the gas phase through stomata, and the root uptake from the soil solution and then the liquid phase transfer in the transpiration streams (Gworek et al. 2016). In our pot experiment, the atmosphere was not contaminated by dust from the B soil, and continuously renewed, likely avoiding foliar exposure.

Pigment contents and chlorophyll fluorescence of the leaves

The total chlorophyll density (Chl) significantly decreased (−26%) for the plants grown in the B soil, as well as the Chl A (−30%) and Chl B (−19%) (Table 4). This matched with the drops of leaf area and water content of the shoots (Table 3) and with some significant changes in the leaf ionome (e.g., increase of foliar Zn, Cu, Cd, and As concentrations; decrease of foliar P and Mg concentrations, Table 5). The excess metal(loid)s and lesser P and Mg concentrations in leaves would impact the chlorophyll biosynthesis (Guo et al. 2016; Kolbas et al. 2018). Instead, the chlorophyll fluorescence remained constant across the soil series;

Table 4 Pigment contents and chlorophyll fluorescence of the tobacco leaves

	Soil treatment (% of B soil)				
Plant parameters	**0**	**25**	**50**	**75**	**100**
Total Chl (mg/m^2)	116 ± 22 **a**	116 ± 14 **a**	94 ± 19 **a**	98 ± 15 **a**	85 ± 7 **b**
ChlA (mg/m^2)	80 ± 17 **a**	80.4 ± 9.9 **a**	63 ± 14 **ab**	67 ± 11 **ab**	56.1 ± 5.8 **b**
ChlB (mg/m^2)	36.7 ± 5.9 **a**	35.9 ± 4.4 **ab**	30.9 ± 5.3 **ab**	32.1 ± 4.9 **ab**	29 ± 2 **b**
ChlA/ChlB	2.18	2.24	2.04	2.09	1.93
Chl FL (Fv/Fm)	0.82 ± 0.02 **a**	0.78 ± 0.07 **a**	0.80 ± 0.06 **a**	0.77 ± 0.06 **a**	0.80 ± 0.02 **a**
Carotenoids (mg/m^2)	10.3 ± 1.7 **a**	10.4 ± 1.2 **a**	9 ± 1 **a**	9.5 ± 1.3 **a**	8.7 ± 1.6 **a**
Total Chl/carotenoids	11.26	11.15	10.44	10.32	9.77

Chl, chlorophyll; *Chl FL*, chlorophyll fluorescence; F_0, minimal fluorescence level in the dark adapted state; *Fm*, maximum fluorescence; *Fv*, $Fm-F_0$; *Fv/Fm*, maximum quantum efficiency of PSII photochemistry. Values are means ± SD (n=4); letters indicate significant differences between treatments for each parameter at p <0.05 (post hoc Tukey HSD test)

Table 5 Ionome of tobacco leaves depending on soil treatments and bioconcentration factors (BCF) for the plants grown on the B soil

	Soil treatment (% of B soil)					**BCF**
Element (mg/kg)	**0**	**25**	**50**	**75**	**100**	
Al	29 ± 2.7 **a**	41.4 ± 14.6 **a**	36 ± 9 **a**	37 ± 11 **a**	39 ± 2 **a**	0.001
As	0.24 ± 0.03 **c**	2.19 ± 0.33 **b**	2.61 ± 0.15 **ab**	2.87 ± 0.35 **ab**	3.42 ± 0.73 **a**	0.041
Cd	0.48 ± 0.05 **d**	0.58 ± 0.08 **d**	0.85 ± 0.12 **c**	1.24 ± 0.13 **b**	1.74 ± 0.09 **a**	0.201
Ca	40,033 ± 2063 **a**	37,618 ± 1948 **a**	37,262 ± 1008 **a**	38,077 ± 1514 **a**	32,445 ± 1021 **b**	0.578
Cr	0.35 ± 0.01 **a**	0.40 ± 0.12 **a**	0.45 ± 0.07 **a**	0.42 ± 0.04 **a**	0.44 ± 0.08 **a**	0.0002
Co	0.12 ± 0.02 **a**	0.13 ± 0.01 **a**	0.13 ± 0.02 **a**	0.31 ± 0.33 **a**	0.28 ± 0.09 **a**	0.001
Cu	17.8 ± 4.2 **b**	20.2 ± 2.1 **ab**	22.2 ± 2.3 **ab**	24.1 ± 3.1 **ab**	27 ± 5 **a**	0.005
Fe	81.2 ± 4.2 **a**	83.1 ± 10.9 **a**	77 ± 10 **a**	164 ± 147 **a**	166 ± 33 **a**	0.001
Mg	7415 ± 981 **a**	5628 ± 705 **b**	5677 ± 450 **b**	5485 ± 376 **b**	5895 ± 503 **b**	0.83
Mn	25.1 ± 2.5 **a**	10.2 ± 0.98 **b**	8 ± 1 **b**	9.5 ± 3.3 **b**	21 ± 5 **a**	0.007
Mo	1.21 ± 0.23 **c**	1.52 ± 0.15 **c**	2.4 ± 0.5 **b**	2.87 ± 0.36 **b**	5.1 ± 0.6 **a**	0.025
Ni	1.35 ± 2.07 **a**	0.43 ± 0.09 **a**	0.57 ± 0.18 **a**	0.76 ± 0.04 **a**	2.49 ± 0.58 **a**	0.008
P	5972 ± 1026 **a**	6226 ± 530 **a**	6470 ± 257 **a**	5649 ± 453 **a**	2861 ± 334 **b**	4.30
Pb	0.96 ± 0.18 **c**	1.5 ± 0.6 **bc**	1.85 ± 0.67 **abc**	3.08 ± 1.35 **ab**	3.45 ± 0.25 **a**	0.001
K	33,565 ± 11,484 **a**	47,091 ± 3009 **a**	44,987 ± 5867 **a**	41,663 ± 1565 **a**	33,438 ± 6028 **a**	5.84
Na	1544 ± 813 **b**	408 ± 133 **b**	384 ± 73.9 **b**	717 ± 180 **b**	4042 ± 1786 **a**	0.44
Zn	60 ± 15 **d**	154 ± 23 **c**	223 ± 27 **c**	329 ± 58 **b**	454 ± 53 **a**	0.008

BCF, foliar element concentration vs. total soil element . Values are means ± SD (n=4); letters indicate significant differences between treatments for each parameter at p <0.05 (post hoc Tukey HSD test)

Table 6 Ionome of tobacco stems depending on soil treatments

	Soil treatment (% of B soil)					**Literature**	**References**
Element (mg/kg DW)	**0**	**25**	**50**	**75**	**100**		
Al	15 ± 4 **a**	20.9 ± 9.9 **a**	16.5 ± 7.6 **a**	21.2 ± 9.3 **a**	14.3 ± 4.5 **a**	92.9–446	1
As	0.11 ± 0.02 **c**	0.44 ± 0.05 **bc**	0.54 ± 0.04 **bc**	0.75 ± 0.13 **ab**	1.1 ± 0.5 **a**		
Cd	0.18 ± 0.04 **b**	0.22 ± 0.03 **b**	0.29 ± 0.05 **b**	0.5 ± 0.1 **a**	0.52 ± 0.09 **a**	1.2–28.6	2
Ca	11,060 ± 1100 **a**	12,526 ± 1701 **ab**	11,084 ± 709 **a**	14,515 ± 1485 **b**	10,808 ± 647 **a**	15,900–11,700	1
Cr	0.21 ± 0.04 **a**	0.32 ± 0.13 **a**	0.30 ± 0.07 **a**	0.33 ± 0.11 **a**	0.28 ± 0.01 **a**		
Co	0.07 ± 0.03 **a**	0.11 ± 0.03 **a**	0.07 ± 0.01 **a**	0.10 ± 0.05 **a**	0.25 ± 0.12 **a**		
Cu	15.7 ± 3.8 **b**	17.2 ± 2.2 **ab**	16.8 ± 1.2 **ab**	21.7 ± 3.5 **ab**	24.5 ± 6.2 **a**	8.2–36.1	1
Fe	58.8 ± 27.3 **a**	97 ± 64 **a**	47.4 ± 14.8 **a**	80 ± 51 **a**	100 ± 35 **a**	168–694	1
Mg	2025 ± 267 **a**	1622 ± 47 **a**	1601 ± 246 **a**	1932 ± 116 **a**	1941 ± 390 **a**	3500–2200	1
Mn	6.29 ± 1.89 **a**	5 ± 1 **a**	3.99 ± 0.05 **a**	5.34 ± 2.15 **a**	7.22 ± 2.35 **a**	25.7–46.6	1
Mo	0.34 ± 0.04 **b**	0.4 ± 0.1 **b**	0.47 ± 0.07 **b**	0.81 ± 0.39 **ab**	1.13 ± 0.37 **a**		
Ni	0.39 ± 0.28 **b**	0.25 ± 0.07 **b**	0.34 ± 0.01 **b**	0.58 ± 0.11 **b**	1.71 ± 0.51 **a**		
P	4047 ± 1043 **a**	4319 ± 474 **a**	4101 ± 214 **a**	4569 ± 523 **a**	2242 ± 161 **b**	3800–2100	1
Pb	0.67 ± 0.31 **b**	1.49 ± 0.65 **ab**	1.11 ± 0.25 **ab**	3.14 ± 1.65 **ab**	2.62 ± 0.61 **a**		
K	21,752 ± 6747 **a**	27,228 ± 3233 **a**	24,870 ± 2325 **a**	26,981 ± 1988 **a**	22,336 ± 2493 **a**	42,700–28,500	1
Na	4523 ± 2225 **ab**	2074 ± 98 **b**	1831 ± 102 **b**	2863 ± 528 **b**	6351 ± 1679 **a**		
Zn	34.3 ± 11.2 **c**	102 ± 18 **bc**	121 ± 10 **b**	216 ± 38 **a**	285 ± 69 **a**	26.8–36.2	1

[1] Tobacco shoots, Kolbas et al. (2020); [2] Tobacco stem, Mench et al. (1989). Values are means ± SD (n=4); letters indicate significant differences between treatments for each parameter at p <0.05 (post hoc Tukey HSD test)

mean Fv/Fm values varying in the 0.77–0.82 range, close to the optimum value (0.83). Carotenoid content was not significantly affected (Table 4). Consequently the Chl vs. carotenoids ratio decreased for the B plants as compared to the Ctrl plants.

Ionome

The foliar and stem concentrations of several elements were affected by the increased proportion of B soil in the soil series (Tables 5 and 6). Foliar As, Cd, Cu, Mo, Pb, and Zn concentrations progressively increased with the addition rate of B soil (Table 5). Highest increases in foliar concentrations were for As (14.2 fold), Zn (7.5 fold), and Mo (4.2 fold) in the B plants as compared to the Ctrl ones. The root uptake of As and Mo oxyanions would be favored by the alkaline soil pH. In contrast, foliar Mg concentrations decreased since the 25% addition rate, and foliar Ca and P concentrations dropped to the 100% one. Foliar Al, Cr, Co, Fe, Ni, and K concentrations did not differ across the soil series. Similarly, stem As, Cd, Cu, Mo, Ni, Pb, and Zn concentrations increased along the soil series and peaked for the B plants, the largest increases being for As (tenfold) and Zn (eightfold) (Table 6). Conversely, stem P concentration decreased for the B plants, stem Na concentration dropped for the 25%, 50%, and 75% addition rates, while stem Al, Ca, Cr, Co, Fe, Mg, Mn, and K concentrations did not significantly vary across the soil series. Foliar As and Zn concentrations were respectively 3 and 1.6 times higher than the stem ones. These changes in leaf and stem ionomes were likely induced by the increase in metal(loid) exposure and the shoot biomass trend to progressively decrease, this one being correlated to the addition rate of B soil ($Y = 0.00008\ X^2 - 0.038\ X + 8.84$, $R^2 = 0.96$; the mineral elements were less diluted in the reduced biomass of aboveground plant parts). Our foliar and stem Cd concentrations were relatively low across the soil series (0.5–1.7 and 0.2–0.5 mg Cd kg^{-1} DW, respectively, Tables 5 and 6) despite the high total soil Cd in the B soil. This likely reflected the low concentration of 1M NH_4NO_3-extractable soil Cd in this B soil (Table 1). In Erdem et al. (2012), the shoot DW yield of tobacco was only decreased over 4.5–6.3 mg Cd kg^{-1} in the shoots depending on genotypes. Cadmium concentration in the leaves and the stem of *N. tabacum* cv. PBD6 respectively reached 6.8 and 1.2 mg kg^{-1} and 164.5 and 28.6 mg kg^{-1} in a control (0.44 mg Cd kg^{-1} DW soil) and Cd-spiked (5.44 mg Cd kg^{-1} DW soil) acid sandy-clay soil (typical of the Bergerac area, France, and usually cultivated with tobacco) without visible phytotoxicity symptom (Mench et al. 1989). Foliar Cu concentration of tobacco plants across the soil series just reached its upper critical threshold range (15–30 mg Cu kg^{-1}, Macnicol and Beckett 1985). Stem Cu concentrations (Table 6) matched with the range of shoot Cu concentrations reported in Kolbas et al. (2020) for the BaG tobacco cultivar grown in field plots with a Cu/PAH-contaminated soil. According to Majsec et al. (2016), Cd and Cu can influence each other uptake, with Cu reducing Cd translocation to tobacco shoots. Cadmium accumulation in the tobacco leaves would depend on a coordination of Cd transport, including less cell wall binding, weaker impediment by the Casparian strip, and efficient xylem loading (Huang et al. 2021). Foliar Zn concentrations for the tobacco plants grown from 50% of B soil (Table 5) exceeded the physiological non-toxic levels reported for most plant species (20–150 mg kg^{-1}). At the Bettwiesen site, Switzerland (total soil Zn 400–55,000 mg Zn kg^{-1}, extractable soil Zn 16 mg Zn kg^{-1}), the BaG tobacco shoots reached up to 617 mg Zn kg^{-1} DW, which was higher than the foliar Zn concentration of tobacco grown on the B soil (Table 5), leading to 20.1 kg Zn ha^{-1} yr^{-1} for shoot Zn removal and a cleanup time of 10 years for the bioavailable Zn stripping (Herzig et al. 2014). At the Lommel site, Belgium (sandy soil, soil pH 6.4–6.8), the shoot concentrations of BaG tobacco reached 250–475 mg Zn and 10–27 mg Cd kg^{-1} DW, Cd being more uptake than at the Borifer site (Thijs et al. 2018). Some papers reported on the root-to-shoot translocation of Zn and Cd in tobacco and Zrt-/Irt-like proteins (ZIPs), which carry Zn from extracellular space and intracellular compartments to the cytosol (Kozak et al. 2019). High Zn and Cd exposures induced changes in root part-specific expression pattern of such membrane transporters, i.e., *NtZIP1-like*, *NtZIP5-like*, *NtZIP8*, *NtZIP11*, *NtIRT1*, and *NtIRT1-like* (Palusińska et al., 2020). The NtZIP11 plasma membrane protein, being highly expressed in tobacco leaves and upregulated by high Zn concentrations (Kozak et al. 2019), may contribute to accumulate Zn in leaves in conditions of Zn excess as in the case of B soil. With high Zn exposure in hydroponic, Zn-containing biogenic calcite and other Zn compounds are produced through the tobacco trichomes, and this would be a mechanism involved in Zn detoxification (Sarret et al. 2006).

The BCF values based on leaf ionome and total soil content culminated for K and P, and then for Mg and Ca (Table 5). For metal(loid)s, the BCF values peaked for Cd, then As and Mo, but in general, these values remained low (< 1) for tobacco plants cultivated in the B soil as compared for instance with values reported by Yang et al. (2017). *Nicotiana tabacum* genotypes are Cd accumulator in general, for example, as compared to *N. rustica* L. (Mench et al. 1989; Herzig et al. 2014; Yang et al. 2017; Huang et al. 2021), but here, the alkaline soil pH in the B soil likely limited the Cd phytoavailability as indicated by the low extractable soil Cd. The BCF value of Zn was lower than that of Cd, but this was due to the high value of total soil Zn and its chemical soil speciation.

A multivariate analysis based on the data of the stem ionome and the other plant parameters (RDA, Fig. 4A) evidenced that on the first component (70% variability explained) were most of the metal(loid) concentrations and the morpho-

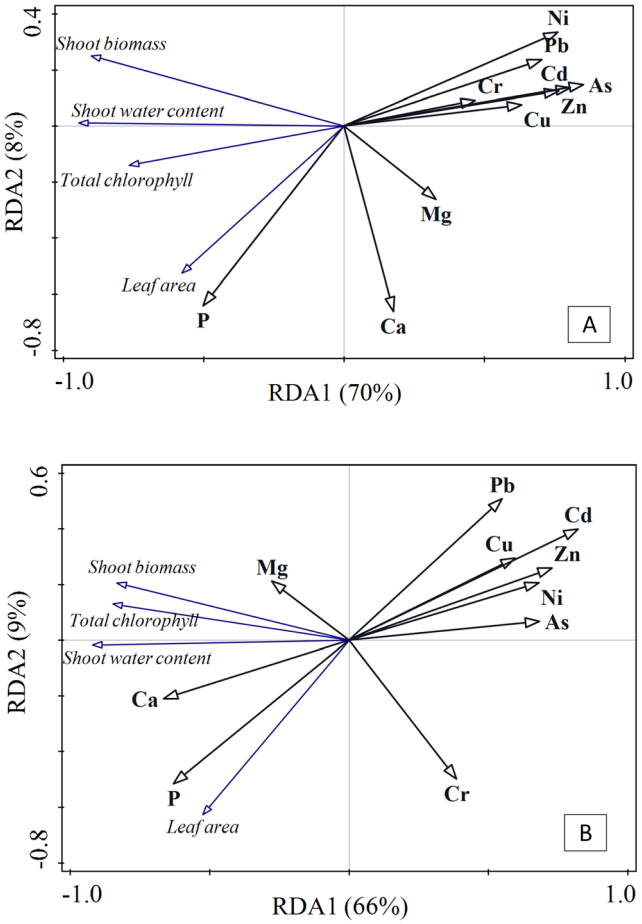

Fig. 4 RDA analysis for shoot biomass, ionome of plant parts, and other plant parameters. **A** Stem ionome. **B** Ionome of leaves

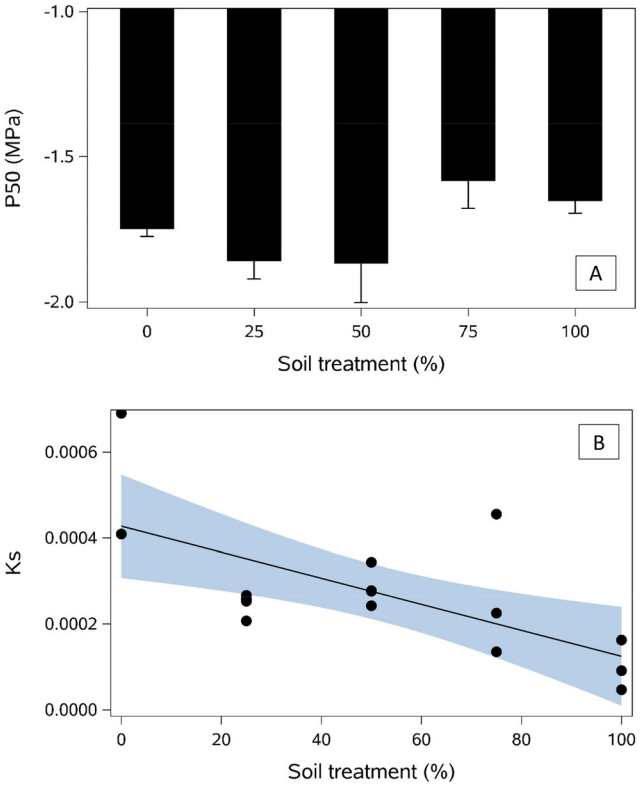

Fig. 5 **A** Vulnerability to drought-induced embolism (hydraulic safety, P50, MPa, differences between mean values were not significant at the 5% level). **B** Specific hydraulic conductance (hydraulic efficiency, Ks, m^2 MPa^{-1} s^{-1}, ■ 95% confidence limits, R^2 =0.43) of tobacco stems depending on soil treatments (% of B soil)

physiological parameters, even though both categories of vectors were in opposite directions. Along the second component (8% variance explained), stem Mg, Ca, and P concentrations and leaf area followed the same direction. The leaf area and stem P concentration were positively correlated, and stem Ca and Mg concentrations as well. This analysis confirmed that as the root exposure to metal(oid)s increased in the soil, so the shoot biomass, the shoot water content, the total chlorophyll, and the leaf area diminished. In contrast, stem P, Ca, and Mg concentrations followed a different trend in comparison to the metal(oid)s, probably because these essential nutrients were present in the soil in sufficient concentrations to satisfy the physiological needs of the plants. The decrease in the ratio of leaf Mg concentration to stem Mg concentration as the soil contamination increased corresponded with the decrease in leaf area and chlorophyll pigments, which could explain a lower demand in Mg, which is a co-factor in the protochlorophyllide, an intermediate in the biosynthesis of chlorophyll *a*.

The same multivariate analysis for the tobacco leaves (RDA, Fig. 4B) indicated similarities in the behavior of the vectors: opposite directions along the first axis (66% variance explained) of most of the metal(loid)s (except Cr) and the morpho-physiological parameters. Conversely, foliar Ca, P, and Mg concentrations were once again mostly along the second axis (8% variance explained) or in between both axes. Most foliar metal(loid) concentrations were negatively correlated with foliar P and Ca concentrations. As for the stems, all the plant parameters were negatively correlated with most foliar metal(loid) concentrations and were positively correlated with the foliar P and Ca concentrations. The position or the Cr vector would reflect its almost constant foliar concentration.

Cavitation

Vulnerability to drought-induced embolism (P50), which is commonly used to characterize drought tolerance across plant species (Choat et al. 2012), can be altered by ion-mediated changes in xylem pit membrane porosity (Cochard et al. 2010). The objective was to quantify the extent to which increased soil contamination and metal(loid) uptake can affect drought tolerance in tobacco. The P50 values varied from −1.45 to −2.15 MPa and did not show any significant differences across the soil series (Fig. 5A, p=0.1263). However,

high P50 values at the 75% and 100% addition rates matched with an increasing trend for stem Mg, Mn, and Na concentrations of the B75 and B plants as compared to those of the B50 plants (Fig. 5A, Table 6). The same results (no significant differences) were obtained for the other three hydraulic safety traits (P_{12}, P_{88}, and slope) with slightly higher slope values for increasing soil contamination. On the contrary, hydraulic efficiency (Ks) declined significantly with increasing soil contamination (Fig. 5B). These patterns can be explained by the fact that a salt solution lead to an immediate increase in hydraulic conductance (Van Leperen et al. 2000) while sap ionic composition does not alter xylem vulnerability to embolism (Cochard et al. 2010).

Chlorophyll fluorescence

Increasing soil contamination in this soil series, including excess metal(loid)s and organic xenobiotics, progressively affected the following tobacco parameters: leaf area, shoot water content, total Chl, Chl A, and Chl B densities, and the Chl A/Chl B and total Chl/carotenoid ratios, notably for the B plants. The capacity of tobacco to keep its photosynthetic system efficient depends on the level of metal(loid) exposure and uptake, Zn stress having less effect than Cd stress on the photosynthetic function of tobacco leaves (Zhang et al. 2020). Here, the Chl fluorescence remained constant and close to the optimum value, which means that the PSII efficiency was almost correct and that this tobacco cultivar can manage the stress caused by the contaminant exposure, maintaining the functionality of its physiological system, while some morphological traits were more disadvantaged.

It is difficult to evidence the most stressful soil contaminants involved, especially since synergies/antagonisms between bioavailable contaminants taken up are possible in the cascade of biological processes. On one hand, the most disturbing changes evidenced in the leaf ionome were probably the increase in Cu and Zn concentrations, the drop of K/Na ratio, and the decrease in P and Mg concentrations (Table 5). Interestingly, the phytoavailability of most metal(loid)s was low in the B soil regarding their total soil concentration. On the other hand, exposure to PAH excess can affect the anatomical structure and architecture of roots and water uptake (Harvey et al. 2002; Kummerova et al. 2013). In the B soil, fluoranthene and then pyrene, benzo(b)fluoranthene, and benzo (g,h,i)perylene to a lesser extent, had the highest concentrations in the B soil (Table 2). Gworek et al. (2016) reported that root uptake from the soil solution occurs for the four- and five-ring PAHs (e.g., pyrene, fluoranthene), and that for three-ring PAHs (e.g., fluorene, phenanthrene, and anthracene) and dicotyledonous plants, both uptake by roots and by leaves would occur. Such PAHs can impact the photosynthetic processes, carbohydrate allocation, and ionome of plant parts and induce an oxidative stress (Kummerova et al. 2013; Dupuy et al. 2015; Tomar and Jajoo 2017). Here, with the aging of organic contaminants in the B soil, it could be assumed that their negative influence is not evident, especially since overall tobacco growth was little affected (Table 3). However future trials at this Borifer site will need to determine the potential PAH transfer to the aboveground biomass.

Potential practical application

This BaG tobacco cultivar can contribute to phytoextract the phytoavailable soil Zn and Cd from the B soil. Shoot Zn and Cd removals computed with the biomass (DW) of leaves and stem and their respective Zn and Cd concentrations (Tables 5 and 6) were 2.35 mg Zn and 7.6 μg Cd $plant^{-1}$. This represented 9% for Zn and 44% for Cd of their 1M NH_4NO_3 extractable amount in the potted B soil. Based on cultural practices, i.e., plant density of 85,000–100,000 ha^{-1} (Sheen 1983), the tobacco phytoextraction would be 199–234 g Zn and 0.65–0.76 g Cd ha^{-1}. Such values were low as compared to the BaG tobacco harvested at the Bettwiesen site (i.e., 20.1 kg ha^{-1} yr^{-1}, with 32.5 t DW ha^{-1} for the shoot biomass, Herzig et al. 2014). Here, due to the 2-month exposure and limited volume of potted B soil that can be explored by the root system, the shoot biomass was only equivalent to 6.04 t DW ha^{-1}. For comparison purposes, soil pH was neutral at the Bettwiesen site (7.1) but 0.1M $NaNO_3$-extractable concentrations (in mg kg^{-1}) were 0.15–55 for Zn and 0.003–0.01 for Cd (Herzig et al. 2014), therefore of the same magnitude order as compared to the Borifer soil (Table 1). Indeed, such bioavailable Zn and Cd stripping and its potential influence on pollutant linkages (e.g., herbivory, Grignet et al. 2020) must be in situ investigated at the Borifer site to get a better assessment. In such sandy soil, it is also possible to harvest the root systems of tobacco, which generally display high Pb and Cu concentrations (Kolbas et al. 2020). Herbivory exposure with tobacco was not evidenced in the field trial at the St-Médard d'Eyrans site (Gironde County, France), except for snails and slugs at the 6–7 leaf stage just after transplanting on site (Kolbas et al. 2020). The resupply of the phytoavailable soil fraction will be regulated by the metal(loid)-bearing solid phases and the soil properties, including the soil pH and Eh. Other Zn/Cd-phytoextraction options are reported in Europe: e.g., *Salix viminalis* L. and *Arabidopsis halleri* (L.) O'Kane & Al-Shehbaz alone and in inter-row co-cropping at the urban Montataire site, Oise County, France (Grignet et al. 2020), *Noccaea caerulescens* (J. Presl & C. Presl) F. K. Mey (Jacobs et al., 2019), short rotation coppice of poplars and willow, and sunflower (Thijs et al. 2018). However, the growth of these plant species would be likely limited by the hot and dry summer weather conditions in southwest France. The black poplars (*Populus nigra* L.) implemented at the Chaban-Delmas site in the Parc aux Angéliques, which is adjacent to the Borifer site, suffered from this and must be

irrigated in the summer (Marchand et al. 2016). The willow and poplar leaves, which accumulate Zn and Cd, are also less easy to harvest. To implement such phytomanagement at this Borifer brownfield, removal of large stones and pieces of concrete, soil loosening, compost incorporation into the soil, and crop irrigation will be crucial points to consider. Winter crops with metal(loid)-excluders, e.g., white clover, alfalfa, and *Festuca* sp., between tobacco cultures would also promote the carbon sequestration, soil fertility, increase in microbial activity, and the biodegradation of organic contaminants (Kidd et al. 2015; Bourceret et al. 2018). Metal(loid) bioavailability may however change with the biodegradation of organic contaminants. Therefore, both must be monitored in parallel to changes in microbial, mesofaunal, and animal communities. Technologies for processing shoot biomass of tobacco harvested at phytomanaged sites are listed in Asad et al. (2017), Yang et al. (2017), Rehman et al. (2019), and Kolbas et al. (2020) and not detailed here. Digestates from anaerobic digestion should not exceed 1000 mg Zn and 1.5 mg Cd kg^{-1} (Arrêté du 8 août, 2019), so this point should be considered regarding the processing of our tobacco biomass. Currently, compost incorporation into the soil combined with hay transfer to promote both the microbial and plant communities is also an option in situ investigated at the Borifer site. As tobacco is grown from May to October in southwest France, soil cover should be provided by a winter crop to avoid soil erosion by natural agents, if possible sequestering carbon and promoting the rhizodegradation of organic contaminants (e.g., alfalfa, white clover, Marchand et al. 2016; Bourceret et al., 2018). If the climatic conditions become drier in summer due to global warming, the cultivation of aromatic plants adapted to the Mediterranean climate should be evaluated (Raveau et al. 2020, 2021).

Conclusion

Growing non-food crops is an option for the phytomanagement and remediation of contaminated soils. Here, the potential ability of tobacco (cv. Badischer Geudertheimer) for phytomanaging a contaminated soil at an urban brownfield site was assessed with a potted soil series made using the fading technique. Despite the high total soil Zn, Cu, Pb, and PAH (e.g., fluoranthene), 2 months after transplantation, the decrease in shoot biomass was only 33% for the plants grown on the undiluted contaminated soil and was not significant as compared to the uncontaminated control soil (Table 3). In contrast, leaf area, water content of shoots, total chlorophyll, and hydraulic efficiency of stem progressively decreased with the soil contamination (Table 3 and Fig. 5). Overall, both foliar and stem Zn and Cd concentrations increased, while the shoot biomass production was roughly maintained, allowing to phytoextract a relevant fraction of the phytoavailable soil Zn and Cd. Few nutrient concentrations in aboveground plant parts decreased with the soil contamination, e.g., foliar and stem P concentrations. This phytomanagement option needs further long-term evaluation on plots at the site, as well as agronomic and bioaugmentation practices that can optimize it and its consequences on soil ecological functions (e.g., changes in microbial and mesofaunal communities, herbivory, organic matter, and contaminant cycles), without underestimating the potential impact of increasingly frequent droughts and heat waves and water availability being a crucial factor for this sandy soil at this brownfield site.

Supplementary Information The online version contains supplementary material available at https://doi.org/10.1007/s11356-021-16411-y.

Acknowledgements The City of Bordeaux (Bordeaux Metropole) has given access to the site and its history. Tobacco seeds were initially provided by Dr. R. Herzig, Phytotech, Bern, Switzerland.

Author contribution All authors read and approved the final manuscript. Set-up and management of the trial, collection and analysis of soil and plant samples, and measures of plant parameters: EDL, MJM, AB, and LM; Metal(loid) speciation in the soils: MPI; Training—measures of chlorophyll fluorescence: RB, EDL, and MJM; Preparation of plant samples and measure of cavitation parameters: GC, MJM, and EDL; Statistical analysis: NO, AB, EDL, and SD; Computation of vulnerability to cavitation: SD; Drafting of the manuscript, data interpretation: MJM, EDL; Contribution to the manuscript writing: MM, MPI, and SD

Funding This work was supported by the BioFoodonMars project (https://projects.au.dk/faccesurplus/research-projects-3rd-call/biofoodonmars/, https://biofoodonmars.com/) funded by the ERA-NET FACCE SURPLUS Cofund 3rd call (https://projects.au.dk/faccesurplus/research-projects-3rd-call/), formed by a partnership of 11 research agencies from 9 countries in the frame of the Joint Programming Initiative on Agriculture, Food Security and Climate Change (FACCE-JPI) with the financial support through two successive Coordination and Support Actions from the European Commission (FACCE CSA - 277610; FACCE-EVOLVE - 652612); the Phy2SUDOE project (SOE4/P5/E1021) under the Interreg SUDOE: "Advancing in the application of innovative phytomanagement strategies in contaminated areas of the SUDOE space" (https://www.phytosudoe.eu/en/); and the Cluster of Excellence COTE (ANR-10-LABX-45) of the French National Agency for Research (Platform project CAVIPLACE).

The UMR BIOGECO is member of the INRAE ecotoxicology network (ECOTOX, https://www6.inrae.fr/ecotox_eng/) and the COST Action 19116 PlantMetals (https://plantmetals.eu/plantmetals-home.html). Eliana Di Lodovico has received a 3-month grant for Traineeship (SMT) from the Erasmus Plus Mobility, The European Commission.

Data availability The datasets used and/or analyzed during the current study are available from the corresponding author on reasonable request.

Declarations

Ethics approval and consent to participate Not applicable

Consent for publication Not applicable

Competing interests The authors declare no competing interests.

References

ADEME (Chateau L), MODAAL Conseil (Milton Y, Petit S) and TESORA (Pauget B, Challaye C) (2018) La reconversion des friches polluées au service du renouvellement urbain : enseignements technico-économiques - Bilan des opérations aidées dans le cadre du dispositif ADEME d'aide aux travaux de dépollution pour la reconversion des friches polluées (période 2010-2016) – Report 125 pages. Available at https://upds.org/wp-content/uploads/2018/12/etude-bilan-travaux-reconversion-friches-polluees-modaal-tesora-2018.pdf. Access on April 16, 2021.

Arrêté du 8 août (2019) approuvant deux cahiers des charges pour la mise sur le marché et l'utilisation de digestats de méthanisation agricole en tant que matières fertilisantes. JORF n°0221 du 22 septembre 2019. Available at https://www.legifrance.gouv.fr/eli/arrete/2019/8/8/AGRG1926797A/jo/texte. Accessed on April 29th, 2021.

Asad M, Menana Z, Ziegler-Devin I, Bert V, Chalot M, Herzig R, Mench M, Brosse N (2017) Pretreatment of trace element-enriched biomasses grown on phytomanaged soils for bioethanol production. Ind Crops Prod 107:63–72. https://doi.org/10.1016/j.indcrop.2017.05.028

Azaizeh H, Castro P M L, Kidd P (2011) Biodegradation of organic xenobiotic pollutants in the rhizosphere. In: Schröder P., Collins C. (eds) Organic xenobiotics and plants. Plant Ecophysiology 8, Springer, Dordrecht. pp 191-215. https://doi.org/10.1007/978-90-481-9852-8_9

Baize (1997) Teneurs totales en éléments traces métalliques dans les sols (France), INRA Editions, Paris, France. 410 p. ISBN13 978–2–7380-0747-6

Bardos RP, Thomas HF, Smith JWN, Harries ND, Evans F, Boyle R, Howard T, Lewis R, Thomas AO, Haslam A (2018) The development and use of sustainability criteria in SuRF-UK's sustainable remediation framework. Sustainability 10:1781. https://doi.org/10.3390/su10061781

Bardos P, Spencer KL, Ward RD, Maco BH, Cundy AB (2020) Integrated and sustainable management of post-industrial coasts. Front Environ Sci 8:86. https://doi.org/10.3389/fenvs.2020.00086

Bisht S, Pandey P, Bhargava B, Sharma S, Kumar V, Sharma KD (2015) Bioremediation of polyaromatic hydrocarbons (PAHs) using rhizosphere technology. Braz J Microbiol 46:7–21. https://doi.org/10.1590/S1517-838246120131354

Blanke MM (1990) Determination of chlorophyll with DMF. Vitic Enol Sci 45:76–78

Bourceret A, Leyval C, Faure P, Lorgeoux C, Cébron A (2018) High PAH degradation and activity of degrading bacteria during alfalfa growth where a contrasted active community developed in comparison to unplanted soil. Environ Sci Pollut Res 25:29556–29571. https://doi.org/10.1007/s11356-018-2744-1

Cambrollé J, Mancilla-Leytón JM, Muñoz-Vallés S, Luque T, Figueroa ME (2012) Zinc tolerance and accumulation in the salt-marsh shrub *Halimione portulacoides*. Chemosphere 86:867–874. https://doi.org/10.1016/j.chemosphere.2011.10.039

Chaney R L (1993) Zinc phytotoxicity. In: Robson A D (ed) Zinc in soils and plants. Developments in plant and soil sciences, 55. Springer, Dordrecht. pp 135-150. https://doi.org/10.1007/978-94-011-0878-2_10

Choat B, Jansen S, Brodribb TJ, Cochard H, Delzon S, Bhaskar R, Bucci SJ, Feild TS, Gleason SM, Hacke UG, Jacobsen AL, Lens F, Maherali H, Martínez-Vilalta J, Mayr S, Mencuccini M, Mitchell PJ, Nardini A, Pittermann J et al (2012) Global convergence in the vulnerability of forests to drought. Nature 491:752–755. https://doi.org/10.1038/nature11688

Cochard H, Damour G, Bodet C, Tharwat I, Poirier M, Améglio T (2005) Evaluation of a new centrifuge technique for rapid generation of xylem vulnerability curves. Physiol Plant 124:410–418. https://doi.org/10.1111/j.1399-3054.2005.00526.x

Cochard H, Herbette S, Hernández E, Hölttä T, Mencuccini M (2010) The effects of sap ionic composition on xylem vulnerability to cavitation. J Exp Bot 61:275–285. https://doi.org/10.1093/jxb/erp298

Cundy A, Bardos P, Puschenreiter M, Mench M, Bert V, Friesl-Hanl W, Müller I, Li X, Weyens N, Witters N, Vangronsveld J (2016) Brownfields to green fields: realising wider benefits from practical contaminant phytomanagement strategies. J Environ Manage 184:67–77. https://doi.org/10.1016/j.jenvman.2016.03.028

Delzon S, Douthe C, Sala A, Cochard H (2010) Mechanism of water-stress induced cavitation in conifers: bordered pit structure and function support the hypothesis of seal capillary-seeding. Plant Cell Environ 33:2101–2111. https://doi.org/10.1111/j.1365-3040.2010.02208.x

Dupuy J, Ouvrard S, Leglize P, Sterckeman T (2015) Morphological and physiological responses of maize (*Zea mays*) exposed to sand contaminated by phenanthrene. Chemosphere 124:110–115 https://doi.org/10.1016/j.chemosphere.2014.11.051

Environment Canada (2010) Canadian Environmental Quality Guidelines. Carcinogenic and other polycyclic aromatic hydrocarbons (Environmental and Human Health Effects). Available online at https://www.ccme.ca/files/Resources/supporting_scientific_documents/pah_soqg_scd_1445.pdf. Accessed on January 5th, 2021.

Erdem H, Kinay A, Ozturk M, Tutus Y (2012) Effect of cadmium stress on growth and mineral composition of two tobacco cultivars. J Food Agric Environ 10(1):965–969

European Parliament (2021) European Parliament resolution of 28 April 2021 on soil protection (2021/2548(RSP)). Available at https://www.europarl.europa.eu/doceo/document/TA-9-2021-0143_EN.html. Access on May 4, 2021.

Grignet A, de Vaufleury A, Papin A, Bert V (2020) Urban soil phytomanagement for Zn and Cd in situ removal, greening, and Zn-rich biomass production taking care of snail exposure. Environ Sci Pollut Res 27:3187–3201. https://doi.org/10.1007/s11356-019-06796-2

Guo W, Nazim H, Liang Z, Yang D (2016) Magnesium deficiency in plants: an urgent problem. Crop J 4:83–91. https://doi.org/10.1016/j.cj.2015.11.003

Gworek B, Klimczak K, Kijeńska M, Gozdowski D (2016) Comparison of PAHs uptake by selected monocotyledones and dicotyledones from municipal and industrial sewage sludge. Environ Sci Pollut Res 23:19461–19470. https://doi.org/10.1007/s11356-016-7130-2

Harvey P, Campanella B, Castro P, Harms H, Lichtfouse E, Schäffner AR, Smrcek S, Werck-Reichhart D (2002) Phytoremediation of polyaromatic hydrocarbons, anilines and phenols. Environ Sci Pollut Res 209:29–47. https://doi.org/10.1065/espr2001.09.084.7

Herzig R, Nehnevajova E, Pfistner C, Schwitzguébel JP, Ricci A, Keller C (2014) Feasibility of labile Zn phytoextraction using enhanced tobacco and sunflower: results of five- and one-year field-scale experiments in Switzerland. Int J Phytoremediation 16:735–754. https://doi.org/10.1080/15226514.2013.856846

Hou D, Al-Tabbaa A, Guthrie P (2014) The adoption of sustainable remediation behaviour in the US and UK: a cross country comparison and determinant analysis. Sci Total Environ 490:905–913. https://doi.org/10.1016/j.scitotenv.2014.05.059

Huang WX, Zhang DM, Cao YQ, Dang BJ, Jia W, Xu ZC, Han D (2021) Differential cadmium translocation and accumulation between *Nicotiana tabacum* L. and *Nicotiana rustica* L. by transcriptome

combined with chemical form analyses. Ecotox Environ Safe 208: 111412. https://doi.org/10.1016/j.ecoenv.2020.111412

INRA LAS (2018). Sols. Méthodes Applicables Aux Sols. Available online at: https://www6.hautsdefrance.inrae.fr/las/Methodes-d-analyse/Sols (December 11, 2020).

Jacobs A, Noret N, Van Baekel A, Liénard A, Colinet G, Drouet T (2019) Influence of edaphic conditions and nitrogen fertilizers on cadmium and zinc phytoextraction efficiency of *Noccaea caerulescens*. Sci Total Environ 665:649–659. https://doi.org/10.1016/j.scitotenv.2019.02.073

Jeannin T, Yung L, Evon P, Labonne L, Ouagne P, Lecourt M, Cazaux D, Chalot M, Placet V (2020) Are nettle fibers produced on metal-contaminated lands suitable for composite applications? Mater Today 31(Supplement 2):S291–S295. https://doi.org/10.1016/j.matpr.2020.01.365

Kidd P, Mench M, Álvarez-López V, Bert V, Dimitriou I, Friesl-Hanl W, Herzig R, Janssen JO, Kolbas A, Müller I, Neu S, Renella G, Ruttens A, Vangronsveld J, Puschenreiter M (2015) Agronomic practices for improving gentle remediation of trace-element-contaminated soils. Int J Phytoremediation 17:1005–1037. https://doi.org/10.1080/15226514.2014.1003788

Kolbas A, Kolbas N, Marchand L, Herzig R, Mench M (2018) Morphological and functional responses of a metal-tolerant sunflower mutant line to a copper-contaminated soil series. Environ Sci Pollut Res 25:16686–16701. https://doi.org/10.1007/s11356-018-1837-1

Kolbas A, Herzig R, Marchand L, Maalouf JP, Kolbas N, Mench M (2020) Field evaluation of one Cu-resistant somaclonal variant and two clones of tobacco for copper phytoextraction at a wood preservation site. Environ Sci Pollut Res 27:27831–27848. https://doi.org/10.1007/s11356-020-09151-y

Kozak K, Papierniak A, Barabasz A, Kendziorek M, Palusińska M, Williams LE, Antosiewic M (2019) NtZIP11, a new Zn transporter specifically upregulated in tobacco leaves by toxic Zn level. Environ Exp Bot 157:69–78. https://doi.org/10.1016/j.envexpbot.2018.09.020

Kummerova M, Zezulka S, Babula P, Váňová L (2013) Root response in *Pisum sativum* and *Zea mays* under fluoranthene stress: morphological and anatomical traits. Chemosphere 90:665–673. https://doi.org/10.1016/j.chemosphere.2012.09.047

Küpper H, Andresen E (2016) Mechanisms of metal toxicity in plants. Metallomics 8:269–285. https://doi.org/10.1039/c5mt00244c

Lichtenhaler H K, Wellburn A R (1983) Determinations of total carotenoids and chlorophylls a and b of leaf extracts in different solvents. Biochem Soc Trans 603rd Meeting Liverpool I1: 591-592.

Macci C, Peruzzi E, Doni S, Masciandaro G (2020) Monitoring of a long term phytoremediation process of a soil contaminated by heavy metals and hydrocarbons in Tuscany. Environ Sci Pollut Res 27: 424–437. https://doi.org/10.1007/s11356-019-06836-x

Macnicol RD, Beckett PHT (1985) Critical tissue concentrations of potentially toxic elements. Plant Soil 85:107–129. https://doi.org/10.1007/BF02197805

Majsec K, Cvjetko P, Tolic S, Tkalec M, Balen B, Pavlica M (2016) Integrative approach gives new insights into combined Cd/Cu exposure in tobacco. Acta Physiol Plant 38:142. https://doi.org/10.1007/s11738-016-2158-y

Marchand L, Mench M (2015) Parc des Angéliques - Quai de Brazza – site BORIFER - 33000 BORDEAUX. Diagnostic de contamination. Report. January. UMR BIOGECO INRA 1202, Ville de Bordeaux, France. 27 p.

Marchand L, Quintela-Sabaris C, Desjardins D, Oustrière N, Pesme E, Butin D, Wicart G, Mench M (2016) Plant responses to a phytomanaged urban technosol contaminated by trace elements and polycyclic aromatic hydrocarbons. Environ Sci Pollut Res 23: 3120–3135. https://doi.org/10.1007/s11356-015-4984-7

Mench M, Tancogne J, Gomez A, Juste C (1989) Cadmium bioavailability for *Nicotiana tabacum* L., *Nicotiana rustica* L. and *Zea mays* L. grown in soil added or non-added with cadmium nitrate. Biol Fertil Soils 8:48–53. https://doi.org/10.1007/BF00260515

Mench M, Oustrière N, Marchand L, Dellise M, Poschenrieder Ch (2017) Phytomanagement of a Cu-contaminated soil with *Erucastrum incanum* (L.) W.D.J. Koch (*Hirschfeldia incana* (L.) Lagr.-Foss). The 14th International Phytotechnologies Conference, September 25-29, Montréal, Canada

Mench MJ, Dellise M, Bes CM, Marchand L, Kolbas A, Le Coustumer P, Oustrière N (2018) Phytomanagement and remediation of Cu-contaminated soils by high yielding crops at a former wood preservation site: sunflower biomass and ionome. Front Ecol Evol 6:123. https://doi.org/10.3389/fevo.2018.00123

Moreira H, Pereira SIA, Mench M, Garbisu C, Kidd P, Castro P (2021) Phytomanagement of metal(loid)-contaminated soils: options, efficiency and value. Front Environ Sci 9:661423. https://doi.org/10.3389/fenvs.2021.661423

Morgun EG, Makarov MI (2011) Use of sodium polytungstate in the granulo-densimetric fractionantion of soil material. Eurasian Soil Sci 44:394–398. https://doi.org/10.1134/S1064229311040077

Ndubueze E U (2018) Potential of five plant species for phytoremediation of metal-PAH-pesticide contaminated soil. Electronic Thesis and Dissertation Repository. 5342. https://ir.lib.uwo.ca/etd/5342

Palusińska M, Barabasz A, Kozak K, Papierniak A, Maślińska K, Antosiewicz DM (2020) Zn/Cd status-dependent accumulation of Zn and Cd in root parts in tobacco is accompanied by specific expression of ZIP genes. BMC Plant Biology 20:37. https://doi.org/10.1186/s12870-020-2255-3

Pammenter NV, Van der Willigen C (1998) A mathematical and statistical analysis of the curves illustrating vulnerability of xylem to cavitation. Tree Physiol 18:589–593. https://doi.org/10.1093/treephys/18.8-9.589

Payá Pérez A, Peláez Sánchez S (2017). European achievements in soil remediation and brownfield redevelopment. Joint Research Centre, the European Commission. doi: 10.2760/91268. Available at https://op.europa.eu/en/publication-detail/-/publication/cd97ae7f-b9f7-11e7-a7f8-01aa75ed71a1/language-en#document-info. Access on April 16, 2021

Petrová S, Rezek J, Soudek P, Vaněk T (2017) Preliminary study of phytoremediation of brownfield soil contaminated by PAHs. Total Environ 599–600:572–580. https://doi.org/10.1016/j.scitotenv.2017.04.163

Prouzova P, Hoskovcova E, Musilova L, Strejcek M, Uhlik O, Demnerova K, Mackova M (2012) The effect of plants and natural compounds on bacterial population in the contaminated soil. In Lovecka P, Novakova M, Prouzova P, Uhlik O (eds), 5th International Symposium on Biosorption and Bioremediation (BioBio), Prague, Czech Republic, June 24-28, pp 60-63.

Raveau R, Fontaine J, Hijri M, Lounès-Hadj Sahraoui A (2020) The culture of clary sage shaped the rhizospheric bacterial communities more strongly than mycorrhizal inoculation in the trace element-contaminated soil - a two-year monitoring field trial. Front Microbiol 11:586050. https://doi.org/10.3389/fmicb.2020.586050

Raveau R, Fontaine J, Bert V, Perlein A, Tisserant B, Ferrant P, Lounès-Hadj Sahraoui A (2021) *In situ* cultivation of aromatic plant species for the phytomanagement of an aged-trace element polluted soil: plant biomass improvement options and techno-economic assessment of the essential oil production channel. Sci Total Environ 789:147944. https://doi.org/10.1016/j.scitotenv.2021.147944

Rehman MZ, Rizwan M, Irfan Sohail M, Ali S, Waris AA, Khalid H, Naeem A, Raza Ahmad H, Rauf A (2019) Opportunities and challenges in the remediation of metal-contaminated soils by using tobacco (*Nicotiana tabacum* L.): a critical review. Environ Sci Pollut Res 26:18053–18070. https://doi.org/10.1007/s11356-019-05391-9

Reinikainen J, Sorvari J, Tikkanen S (2016) Finnish policy approach and measures for the promotion of sustainability in contaminated land management. J Environ Manage 184:108–119. https://doi.org/10.1016/j.jenvman.2016.08.046

Rezek J, Macek T, Mackova M, der Wiesche CI, Zadrazil F (2004) The effect of vegetation on decrease of PAH and PCB content in long-term contaminated soil. In: Verstraete W (ed) European Symposium on Environmental Biotechnology ESEB 2004, April 25-28. Oostende, Belgium, pp 833–837

Richer De Forges A (2020). Base de données du Référentiel Régional Pédologique du département de la Gironde à 1/250 000. Available at 10.15454/6BX5D7, Portail Data INRAE, V1.

Rizzo E, Bardos P, Pizzol L, Critto A, Giubilato E, Marcomini A, Albano C, Darmendrail D, Döberl G, Harclerode M, Harries N, Nathanail P, Pachon C, Rodriguez A, Slenders H, Smith G (2016) Comparison of international approaches to sustainable remediation. J Environ Manage 184:4–17. https://doi.org/10.1016/j.jenvman.2016.07.062

Saleem MH, Ali S, Hussain S, Kamran M, Chattha MS, Ahmad S, Aqeel M, Rizwan M, Aljarba NH, Alkahtani S, Abdel-Daim MM (2020a) Flax (*Linum usitatissimum* L.): A potential candidate for phytoremediation? Biological and economical points of view. Plants (Basel) 9(4):496. https://doi.org/10.3390/plants9040496.

Saleem MH, Ali S, Rehman M, Hasanuzzaman M, Rizwan M, Irshad S, Shafiq F, Iqbal M, Alharbi BM, Alnusaire TS, Qari SH (2020b) Jute: a potential candidate for phytoremediation of metals—a review. Plants (Basel). 9(2):258. https://doi.org/10.3390/plants9020258

Salt DE, Baxter I, Lahner B (2008) Ionomics and the study of the plant ionome. Annu Rev Plant Biol 59:709–733. https://doi.org/10.1146/annurev.arplant.59.032607.092942

Sarret G, Harada E, Choi Y-E, Isaure M-P, Geoffroy N, Fakra S, Marcus MA, Birschwilks M, Clemens S, Manceau A (2006) Trichomes of tobacco excrete zinc as zinc-substituted calcium carbonate and other zinc-containing compounds. Plant Physiol 141:1021–1034. https://doi.org/10.1104/pp.106.082743

Sheen SJ (1983) Biomass and chemical-composition of tobacco plants under high-density growth. Beitr Z Tabakforsch Int 12:35–42. https://doi.org/10.2478/cttr-2013-0523

Sun Y, Li H, Guo G, Semple KT, Jones KC (2019) Soil contamination in China: current priorities, defining background levels and standards for heavy metals. J Environ Manage 251:109512. https://doi.org/10.1016/j.jenvman.2019.109512

Thijs S, Witters N, Janssen J, Ruttens A, Weyens N, Herzig R, Mench MJ, Van Slycken S, Meers E, Meiresonne L, Vangronsveld J (2018) Tobacco, sunflower and high biomass SRC clones show potential for trace metal phytoextraction on a moderately contaminated field site in Belgium. Front Plant Sci 9:1879. https://doi.org/10.3389/fpls.2018.01879

Tomar RS, Jajoo A (2017) PSI becomes more tolerant to fluoranthene through the initiation of cyclic electron flow. Funct Plant Biol 44:978–984. https://doi.org/10.1071/FP17121

Urli M, Porté AJ, Cochard H, Guengant Y, Burlett R, Delzon S (2013) Xylem embolism threshold for catastrophic hydraulic failure in angiosperm trees. Tree Physiol 33:672–683. https://doi.org/10.1093/treephys/tpt030

USEPA (2021) Search for superfund sites where you live. National Priorities List and Superfund 38 Alternative Approach Sites. Available online at: https://www.epa.gov/superfund/search-superfund-sites-where-you-live#npl. Accessed April 16, 2021.

Van Ieperen W, Van Meeteren U, Van Gelder H (2000) Fluid ionic composition influences hydraulic conductance of xylem conduits. J Exp Botany 51:769–776. https://doi.org/10.1093/jexbot/51.345.769

Verdejo J, Ginocchio R, Sauvé S, Mondaca P, Neaman A (2016) Thresholds of copper toxicity to lettuce in field-collected agricultural soils exposed to copper mining activities in Chile. J Soil Sci Plant Nutr 16:154–158. https://doi.org/10.4067/S0718-95162016005000011

Villanneau EJ, Saby NPA, Orton TG, Jolivet CC, Boulonne L, Caria G, Barriuso E, Bispo A, Briand O, Arrouays D (2013) First evidence of large-scale PAH trends in French soils. Environ Chem Lett 11:99–104. https://doi.org/10.1007/s10311-013-0401-y

Xue K, Zhou J, Van Nostrand JD, Mench M, Bes C, Giagnoni L, Arenella M, Renella G (2018) Functional activity and functional gene diversity of a Cu-contaminated soil remediated by aided phytostabilization using compost, dolomitic limestone and a mixed tree stand. Environ Pollut 242:229–238. https://doi.org/10.1016/j.envpol.2018.06.057

Yang Y, Ge YC, Zeng HY, Zhou XH, Peng L, Zeng QR (2017) Phytoextraction of cadmium-contaminated soil and potential of regenerated tobacco biomass for recovery of cadmium. Sci Rep 7:7210. https://doi.org/10.1038/s41598-017-05834-8

Zhang HH, Xu ZS, Guo KW, Huo YZ, He GQ, Sun HW, Guan YP, Xu N, Yang W, Sun GY (2020) Toxic effects of heavy metal Cd and Zn on chlorophyll, carotenoid metabolism and photosynthetic function in tobacco leaves revealed by physiological and proteomics analysis. Ecotoxicol Environ Saf 202:110856. https://doi.org/10.1016/j.ecoenv.2020.110856